

# Comparative Performance of P&O, Incremental Conductance and Fuzzy MPPT Techniques in Grid-Connected Five-Level Multilevel Inverters with Reduced Switching Devices

Patel Nikunj N <sup>1</sup>, Rakeshkumar A. Patel <sup>2</sup>

<sup>1</sup>Research Scholar, Electrical Engineering Department, U. V. Patel College of Engineering, Ganpat University, Mehsana, India

<sup>2</sup> Professor, Electrical Engineering Department, SPCE, Visnagar, SPU University, Mehsana, India.

## ARTICLE INFO

## ABSTRACT

Received: 18 Dec 2024

Revised: 10 Feb 2025

Accepted: 28 Feb 2025

**Introduction:** This paper presents a comparative performance analysis of three Maximum Power Point Tracking (MPPT) techniques—Perturb and Observe (P&O), Incremental Conductance (INC), and Fuzzy Logic Controller (FLC)—for a grid-connected photovoltaic (PV) system integrated with a five-level multilevel inverter featuring reduced switching devices. The system is modeled and simulated in PSIM under variable irradiance conditions to assess the efficiency and responsiveness of each MPPT method in real-time solar environments. The five-level inverter topology is optimized to minimize the number of switching components while maintaining high-quality output, reduced total harmonic distortion (THD), and effective grid compliance. Each MPPT algorithm is implemented individually and evaluated in terms of dynamic response, convergence time, tracking accuracy, and overall power delivery performance. Simulation results show that while P&O and INC provide reliable and simple control, the fuzzy logic approach outperforms both in handling rapid irradiance fluctuations and reducing steady-state oscillations. The study provides valuable insights for selecting suitable MPPT strategies in advanced PV systems employing multilevel inverters with optimized switch count.

**Keywords:** T-type multilevel inverter, Total Harmonic Distortion, Pulse Width Modulation, Multilevel Inverter, Maximum Power Point Tracking

## INTRODUCTION

As global electricity demand continues to rise and conventional power generation methods become less dominant, photovoltaic inverters are gaining increased attention. A key advancement in power electronics is the development of single-stage converters with a reduced number of switching devices, designed for direct grid connection. These innovative topologies represent a significant leap forward, especially in an era where energy efficiency and grid stability are paramount. By simplifying energy conversion and minimizing switching operations, these converters not only reduce power losses but also enhance system reliability.

The adoption of such converters is crucial for integrating renewable energy sources—like solar and wind—into existing grid infrastructure. In contrast to conventional multi-stage converters that involve complex switching operations, the single-stage design streamlines energy transformation, making systems more efficient and robust. This study aims to thoroughly explore the advantages and impact of these grid-connected, low-switch-count converters, particularly in terms of grid integration, energy efficiency, and renewable energy utilization. This converter technology signifies a substantial stride toward building safer and more dependable energy networks and aligns with recent advancements in power electronics that demand deeper analysis and understanding.

Multilevel inverters are especially beneficial for grid-connected photovoltaic applications. They offer higher efficiency, lower harmonic distortion, better voltage regulation, and reduced electromagnetic interference, making them ideal for scalable solar systems. These advantages support the growing demand for sustainable energy and reliable grid integration.

Small-scale rooftop PV systems, typically rated below 10 kW, have reached a mature stage in both technological development and market availability. Common topologies for such systems include string inverters, multi-string architectures, and AC modules. Widely adopted commercial inverter types include single-phase NPC, H-5, H-6, and HERIC transformerless configurations. These three-level voltage-source inverters are known for their efficient energy conversion.

The H-5 topology, a variant of the H-bridge, introduces an extra DC-side switch to block reactive power flow between the DC-link capacitor and the grid, thereby enhancing system efficiency. Similarly, the H-6 design incorporates a pair of such switches for the same purpose. In the HERIC inverter, a bidirectional bypass switch is placed at the grid connection point to shunt the H-bridge and restrict reactive power flow.

Recent developments also include commercial introduction of five-level NPC H-bridge inverters and cascaded H-bridge designs consisting of two series-connected H-bridge cells. Despite promising literature, H-bridge-based solutions are not yet widely commercialized. Additionally, the market offers transformerless two-stage topologies incorporating high-frequency isolated DC–DC converters. These HF transformers serve both isolation and voltage boosting functions while being more compact than conventional line-frequency transformers. However, these two-stage solutions often result in greater power losses compared to transformerless single-stage configurations.

### MULTILEVEL INVERTER

Minimizing the switching count in an MLI entails reducing the frequency at which switching devices, such as transistors or thyristors, change their states during operation. Multilevel inverters provide an output voltage by integrating various levels of DC voltages, usually using numerous power semiconductor switches organized in a certain arrangement. Every switching event requires the activation or deactivation of one or more of these switches to obtain the intended output voltage waveform.

The efficiency of the converter plays a significant role in determining the market. Converters with greater efficiencies were chosen because of their effective parameters. The efficiency of the two-level inverter increases with an increase in switching frequency. The below Fig.1 represent efficiency and switching frequency.

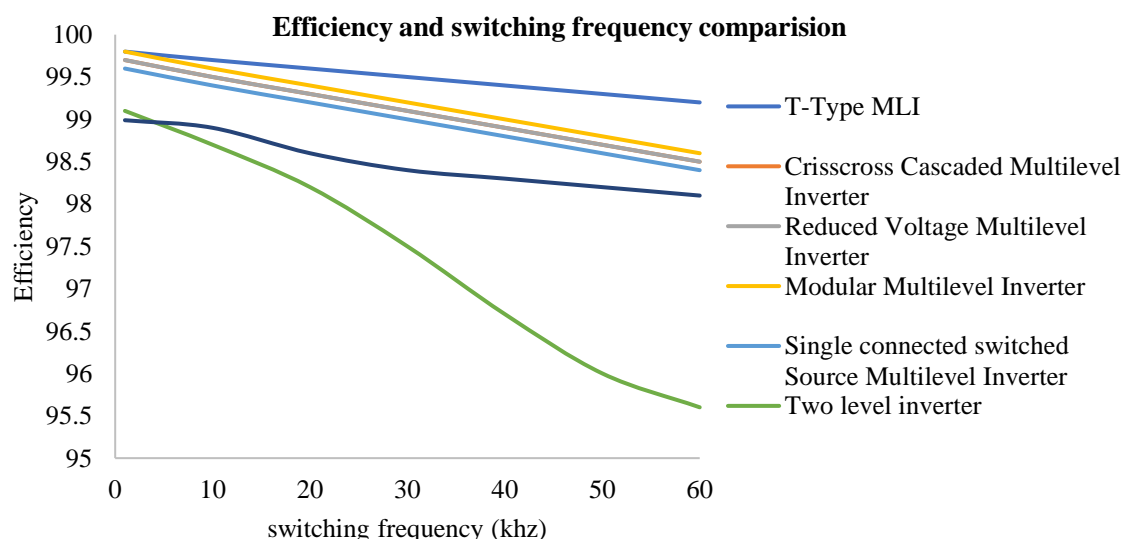


Figure 1. Converter efficiency vs switching frequency

To create a topology that significantly reduces the number of devices required. The number of switch counts for these MLIs increases proportionally, considering the number of levels. An increase in the number of switches requires the addition of additional drivers, isolation circuits, and band circuits, along with necessary heat sinks and protection. In addition, a higher number of switches further amplifies the computational load on the controller. Consequently, when

the levels grow, conventional MLIs experience escalation in size, cost, and complexity, resulting in a costly inverter that presents practical implementation challenges and restricts market penetration.

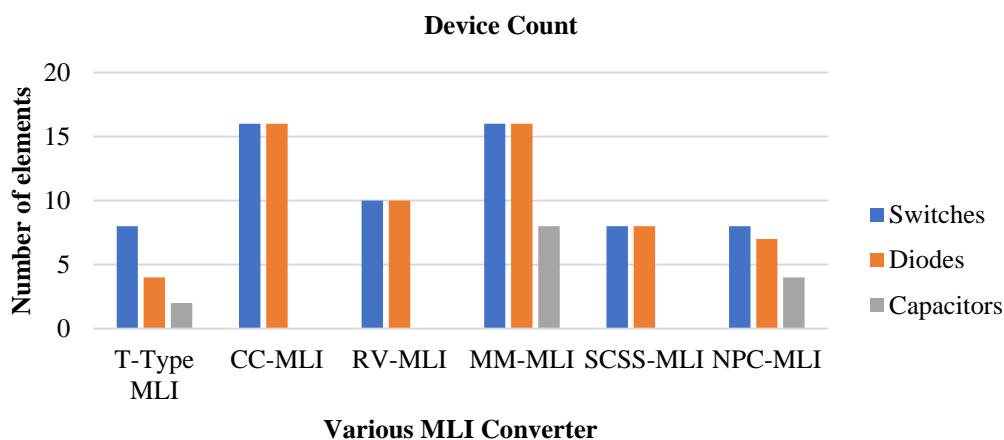
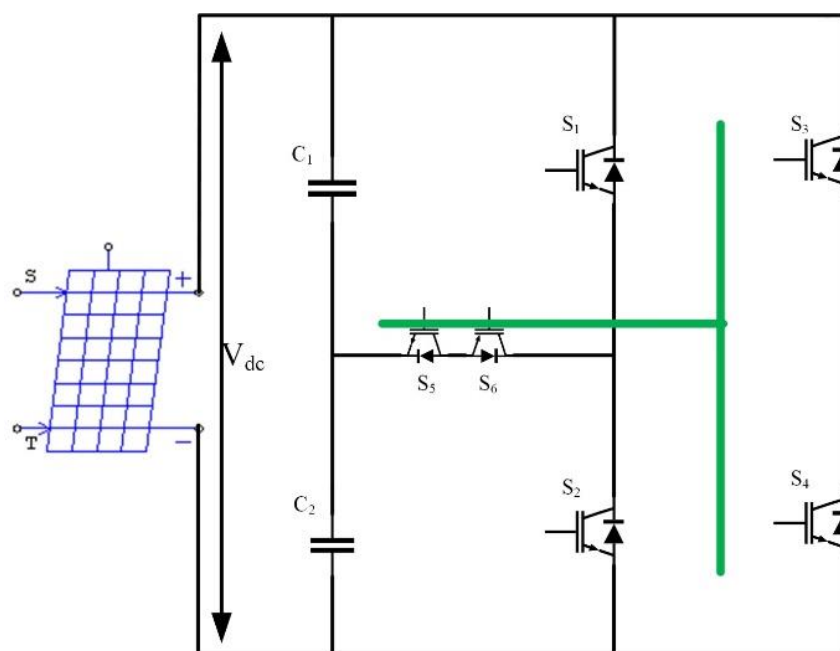


Figure. 2. MLI converter device count with number of elements

### FIVE LEVEL T HYBRID CONVERTER

The device depicted in Figure 3, referred to as the 5 L-T converter, is capable of producing five distinct voltage levels as its output. The bridge configuration comprises a T-type converter leg and half-bridge leg, which are linked to a solitary PV string or array. Therefore, it can perform a single Maximum Power Point tracking operation. Only two redundant states can produce a zero-voltage level. Recurring states are employed to attain voltage equivalence across the dc-link capacitors. The two converter legs create a bridge that enables a direct connection to the dc-link. Hence, it is imperative for the grid to precisely manage both active and reactive powers. Because the dc-link voltage required by the PV strings is half of that required by the 3 L-T converter, they can be scaled in a similar way to the 5 L-TC. The notable characteristic of the converter is that each leg operates at an independent switching frequency. Compared to the higher switching frequency of the 3 L-T cell, the fundamental frequency of the half-bridge cell is equal to the frequency of the grid.



Output Voltage	S1	S2	S3	S4	S5	S6
+Vdc	1	0	1	0	0	0
+Vdc/2	0	0	1	0	1	0
0	0	0	1	1	0	0
-Vdc/2	0	0	0	1	0	1
-Vdc	0	1	0	1	0	0

Figure. 3 Five level T MLI power topology and switching stages

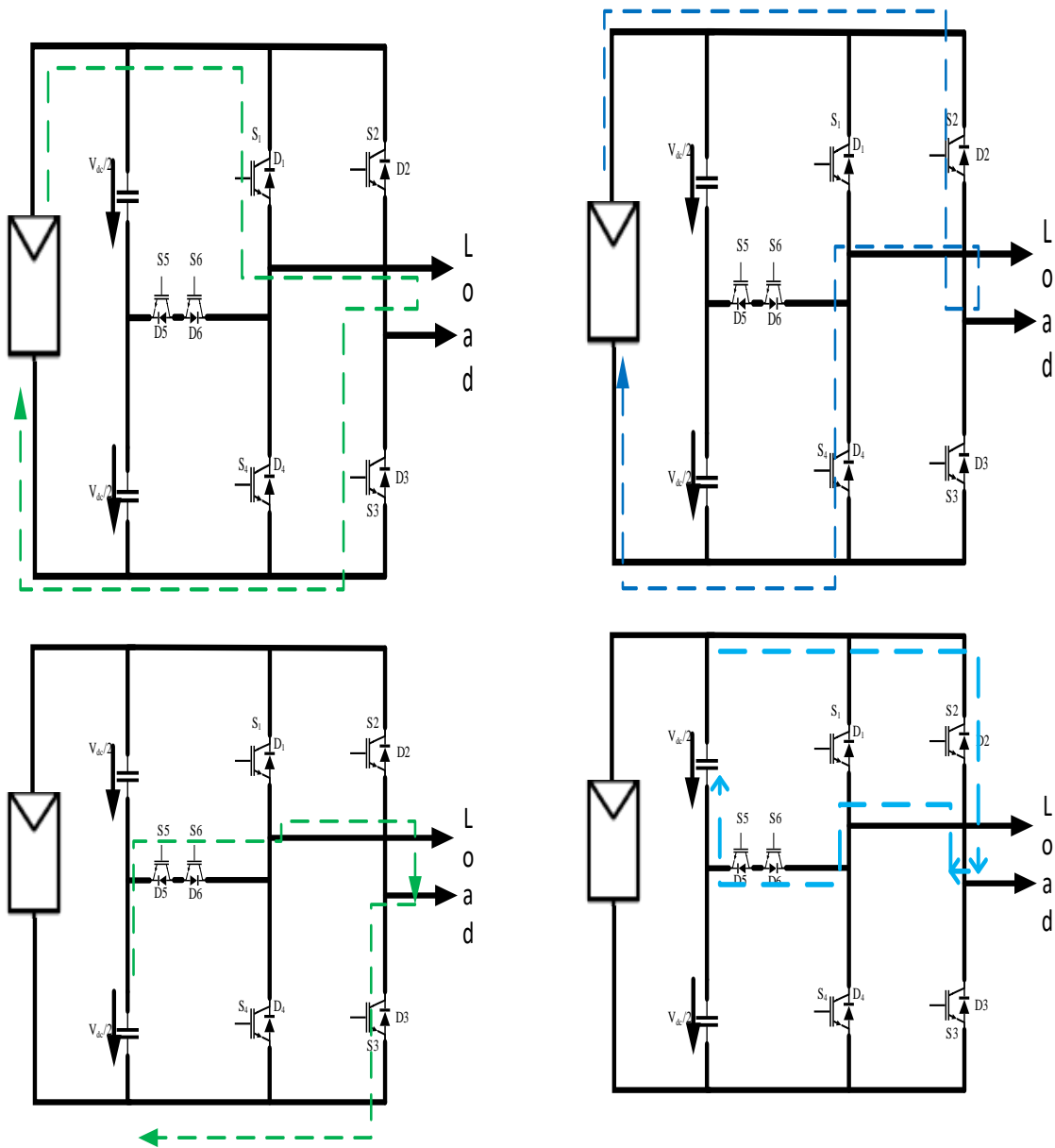


Figure. 4Five level T MLI Operating Stages

Figurer 4 shows the different operational modes in the four stages, each of which is presented sequentially. To begin, power is transferred from the source to the load when the DC source switch S1 is turned on. The current travels from the load back to the generator via S3. The stage received power from the source at its maximum capacity. In the second operational mode, the current flow from the source to the load was established via switches S3, S5, and D6. During the two operational intervals described earlier, the loads underwent a positive half-cycle to initiate a current flow. The load also experienced a negative current flow for the duration of the remaining operating mode

### MPPT IMPLEMENTATION CONTROL TECHNIQUES

In photovoltaic systems, there exists a unique operating point known as the Maximum Power Point, where the product of voltage and current is maximized, yielding maximum power at a voltage VMPP. However, due to the nonlinear I–V characteristics of PV modules and their strong dependence on irradiance and cell temperature, the power output constantly varies. This makes Maximum Power Point Tracking essential to ensure that the PV system operates efficiently under all environmental conditions.

As irradiance increases (e.g., from 400 to 1000 W/m<sup>2</sup>) at constant temperature, both the PV current and voltage increase, resulting in higher output power. In contrast, as temperature rises (e.g., from 25°C to 75°C) under constant irradiance, the current increases slightly while voltage decreases significantly, causing a reduction in output power.

To adapt to these dynamic conditions, MPPT controllers are deployed between the PV generator and the load to continuously adjust the operating point close to the MPP. Traditional algorithms such as Perturb and Observe (P&O) and Incremental Conductance are widely used due to their simplicity and real-time implementation capabilities. However, both have limitations, particularly under rapidly changing weather conditions, where they may fail to converge accurately to the true MPP or cause oscillations.

To overcome these challenges, Fuzzy Logic-based MPPT has emerged as a powerful alternative. It does not require an exact mathematical model and can handle uncertainties and nonlinearity effectively. The fuzzy controller uses linguistic rules and membership functions to decide the optimal changes in duty cycle based on inputs such as changes in power and voltage. As a result, it offers faster convergence, smoother tracking, and better performance under variable atmospheric conditions.

In this study, a comparative analysis of P&O, INC, and Fuzzy Logic MPPT algorithms is conducted using a grid-connected five-level multilevel inverter to evaluate their performance in maximizing energy extraction under different irradiance and temperature conditions.

The Perturb and Observe algorithm is one of the most commonly employed MPPT techniques in photovoltaic systems due to its simplicity and ease of implementation shown in figure 5. The core principle of this method involves periodically measuring the PV array voltage and current to calculate the instantaneous power. At each sampling interval, the present power  $P(t)$  is calculated as the product of the measured voltage  $V(t)$  and current  $I(t)$ , while the previous power  $P(t-\Delta t)$  is computed using delayed values. The algorithm then determines the changes in power ( $\Delta P$ ) and voltage ( $\Delta V$ ) between the two intervals. Based on the signs of these changes, the reference voltage  $V_{ref}$  is adjusted to track the Maximum Power Point. If  $\Delta P = 0$ , the system is assumed to be at or near the MPP, and no action is taken. If  $\Delta P > 0$ , it indicates that the system is moving toward the MPP. In this case, if  $\Delta V > 0$ , the reference voltage is increased, and if  $\Delta V < 0$ , the reference voltage is decreased. Conversely, if  $\Delta P < 0$ , the system is moving away from the MPP, and the reference voltage is adjusted in the opposite direction. This iterative process continues until the PV array operates at or near the MPP. Despite its widespread use, the P&O method may exhibit oscillations around the MPP and reduced tracking accuracy under rapidly changing environmental conditions.

The Incremental Conductance shown in figure 6 algorithm improves upon the limitations of the Perturb and Observe method by using the derivative of power with respect to voltage to locate the Maximum Power Point. Based on the principle that the derivative of power  $dP/dV$  is zero at MPP, positive on the left side, and negative on the right side of the power-voltage curve, this method compares the incremental conductance  $\Delta I/\Delta V$  to the instantaneous conductance  $-I/V$ . If the two values are equal, the operating point is at MPP. If the incremental conductance is greater than the instantaneous conductance, the system increases the operating voltage, and if it is less, the voltage is

decreased. The INC algorithm offers better performance under rapidly changing irradiance conditions compared to P&O, as it can distinguish between changes due to environmental variations and those due to MPPT tracking. However, its implementation is slightly more complex due to the need for derivative calculations.

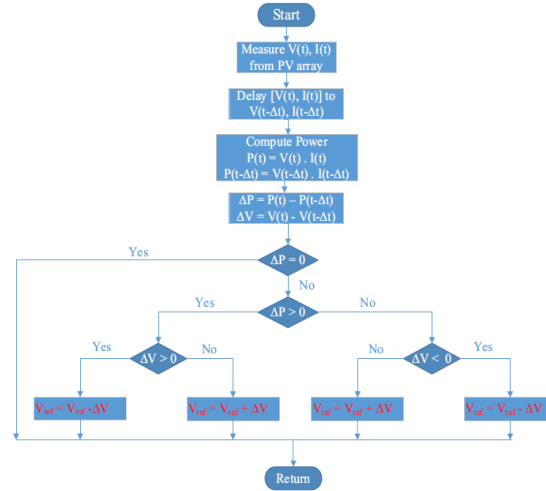


Figure. 5 Flowchart of the P&O algorithm

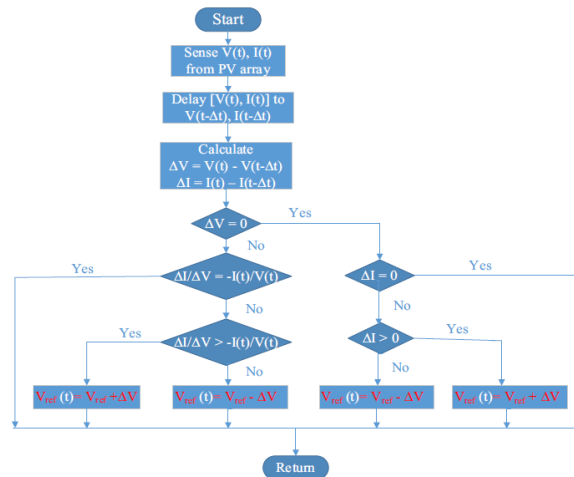


Figure. 6 Flowchart of the INC algorithm

The Fuzzy Logic Controller shown in figure 7 approach for MPPT is designed to handle the nonlinear and time-varying nature of photovoltaic systems without relying on an exact mathematical model. It uses linguistic rules and fuzzy sets to map the input variables—typically the change in power  $\Delta P$  and the change in voltage  $\Delta V$ —to an output that adjusts the duty cycle or reference voltage. The fuzzy inference process involves three key stages: fuzzification of inputs, application of fuzzy rules, and defuzzification of the output to generate a precise control signal. This intelligent decision-making structure allows FLC to respond quickly and smoothly to varying environmental conditions, making it highly effective in maintaining stable and optimal operation near the MPP. Compared to conventional methods, FLC offers superior dynamic response, reduced oscillations, and higher energy yield, particularly under partially shaded or rapidly fluctuating irradiance conditions. However, it requires careful tuning of membership functions and rule sets for optimal performance.

Research Article

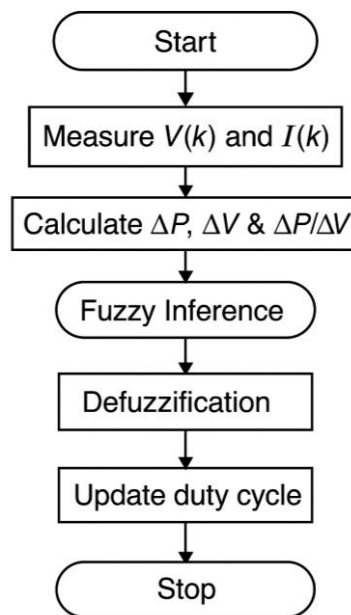
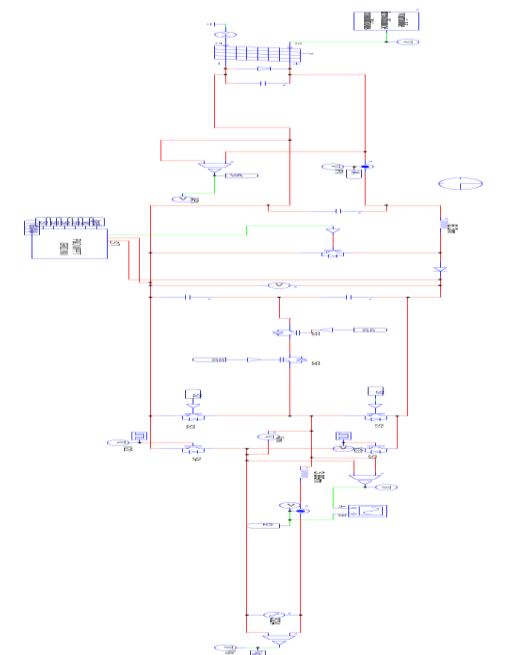


Figure. 7 Flowchart of the Fuzzy algorithm

SIMULATION RESULT & DISCUSSION

A simulation of a 2 kW, 230 V AC single-phase grid-connected system using a T-type multilevel inverter is shown in figure 8 to developed & analyze the performance of advanced inverter topologies under practical operating conditions. The system integrates a DC source, representing a solar photovoltaic array or battery, which is interfaced with the grid through a five-level T-MLI. The inverter topology improves the quality of the output waveform by generating multiple voltage levels, reducing total harmonic distortion and enhancing grid compliance. The control strategy includes a voltage-oriented control scheme combined with a maximum power point tracking algorithm to ensure efficient energy transfer and dynamic response under varying load and irradiation conditions. Simulation results demonstrate the inverter’s ability to deliver clean sinusoidal output with improved efficiency and power quality, making it suitable for residential grid-tied applications.





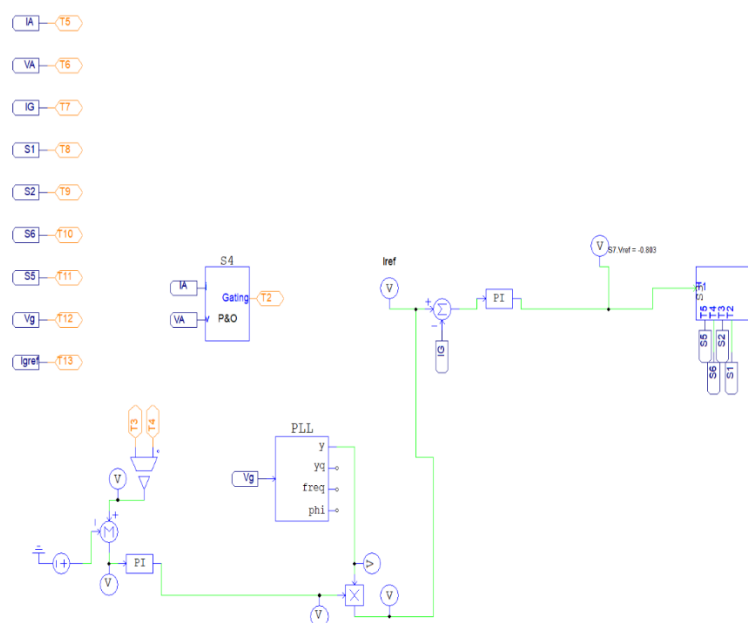


Figure. 8 Simulation of PV with grid inverter

The Figure. 9 illustrates the performance of a photovoltaic system equipped with an MPPT controller under step changes in solar irradiance. The green curve denotes the step changes in irradiance ( $\text{W}/\text{m}^2$ ), while the red curve represents the PV output power, calculated as the product of PV current and voltage. Initially, with irradiance held constant at  $1000 \text{ W}/\text{m}^2$ , the power output rises sharply and stabilizes, reflecting accurate and fast MPPT convergence. As the irradiance drops in steps to  $850 \text{ W}/\text{m}^2$  and further to  $400 \text{ W}/\text{m}^2$ , the output power correspondingly decreases, confirming that the system adapts to the available solar energy and successfully tracks the new MPPs. From 6 seconds onward, as irradiance gradually increases back to  $1000 \text{ W}/\text{m}^2$ , the power output also increases proportionally, again demonstrating the MPPT algorithm's dynamic capability.

This behavior indicates that the employed MPPT algorithm is not only stable but also exhibits fast tracking and minimal oscillation around the MPP, which are critical for maintaining optimal system efficiency. The simulation also reflects the inverter's ability to regulate power smoothly without significant overshoot or delay, making it suitable for grid-connected applications. The system's effectiveness under such transient conditions is essential for real-world PV installations, where irradiance fluctuates due to cloud movement, shadows, or seasonal variations. Thus, the plotted response validates both the reliability of the T-type multilevel inverter and the precision of the MPPT strategy in maximizing energy harvesting from the PV source.

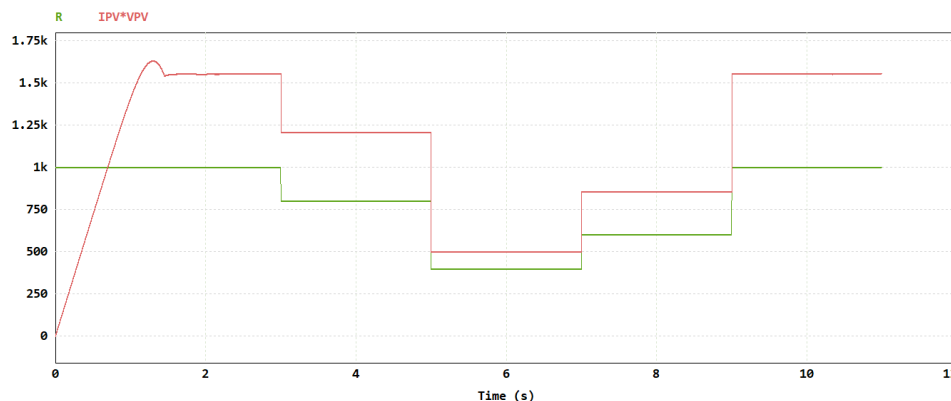


Figure. 9 Solar radiation and Tracked Power



This figure 10.provides a comprehensive overview of the dynamic response of a single-phase grid-connected PV system employing a T-type multilevel inverter under variable irradiance conditions. The first subplot displays the PV voltage and the boosted output voltage . The VPV remains nearly constant, while the boost converter maintains a steady Vboostout slightly above VPV, ensuring proper DC-link voltage for inverter operation. The second subplot shows the grid current , where the amplitude variation reflects the changes in irradiance and power injected into the grid. It also indicates the sinusoidal nature of the current, implying proper synchronization with the grid voltage.

In the third subplot, the inverter output voltage is shown with a five-level staircase waveform, characteristic of the T-MLI topology. This waveform indicates reduced harmonic distortion and efficient voltage synthesis. The fourth subplot depicts the PV output power ( $IPV \cdot VPV$ ), which changes in steps corresponding to irradiance variations. The system demonstrates a fast and smooth power response, validating the effectiveness of the MPPT and control strategy.

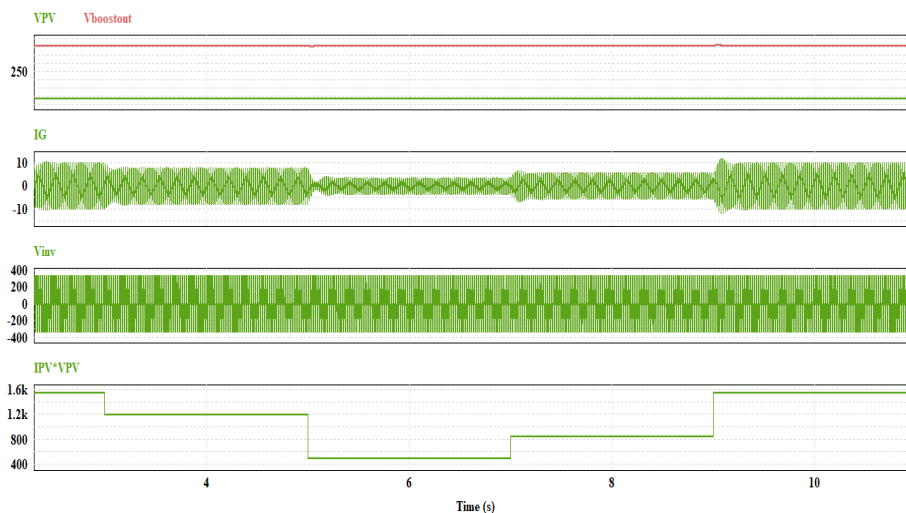


Figure. 10 PV panel voltage,grid current and tracked power

Overall, the simulation confirms stable system operation, fast MPPT tracking, efficient DC-DC conversion, and proper inverter voltage modulation. The grid current waveform and its adaptation to power levels show compliance with grid codes and efficient energy transfer, making the configuration suitable for residential or small commercial applications.

A comparative evaluation of three widely used MPPT techniques Perturb and Observe , Incremental Conductance and Fuzzy Logic Control was conducted under standard test conditions (irradiance of  $1000 \text{ W/m}^2$  and temperature of  $25^\circ\text{C}$ ). The FLC method demonstrated the fastest response time of  $10 \mu\text{s}$ , followed by INC at  $16 \mu\text{s}$  and P&O at  $20 \mu\text{s}$ , indicating that intelligent control methods offer superior tracking speed. In terms of tracked output power, FLC again outperformed the others, achieving  $1558 \text{ W}$ , slightly higher than INC ( $1555 \text{ W}$ ) and P&O ( $1551 \text{ W}$ ). This performance shows that the FLC method is not only faster but also more precise in locating the maximum power point (MPP), making it highly suitable for dynamic environmental conditions in real-world PV applications. The summary is presented in Table 1.

MPPT Technique	Response time(s)	Tracked Power ( $E=1000\text{W/m}^2$ , and $T=25^\circ\text{C}$ )
P&O	20usec	1551 W
INC	16usec	1555 W
FLC	10usec	1558 W

Table.1 Comparision of MPPT technique

The table presents the grid-side electrical performance of a PV system under varying irradiance conditions  $1000 \text{ W/m}^2$ ,  $600 \text{ W/m}^2$ , and  $400 \text{ W/m}^2$ . As expected, panel power output decreases significantly with reduced irradiance, dropping from  $1551 \text{ W}$  at  $1000 \text{ W/m}^2$  to  $855 \text{ W}$  and  $498 \text{ W}$  at  $600 \text{ W/m}^2$  and  $400 \text{ W/m}^2$  respectively. Despite the change in irradiance, the boost converter consistently maintains the DC-link voltage near  $329\text{--}330 \text{ V}$ , and the AC output voltage remains stable around  $238\text{--}239 \text{ V}$ , demonstrating effective regulation by the power conversion system. The RMS current proportionally decreases with reduced power, aligning with the lower energy fed into the grid.

Irradiance conditions	Panel Power	Vboost	Vrms	Irms	V <sub>THD</sub>	I <sub>THD</sub>
1000	1551W	330 V	238 V	6.69 A	28%	4.2 %
400	498 W	329 V	239 V	2.14 A	29%	4.5%
600	855 W	329 V	239 V	3.7 A	29.5 %	4.9 %

Table.2 Grid nparametres for different radiation

Furthermore the voltage total harmonic distortion  $V_{\text{THD}}$  increases slightly from 28% to 29.5% as irradiance decreases, while current  $I_{\text{THD}}$  rises from 4.2% to 4.9%. This trend is indicative of reduced waveform quality at lower power levels, which is common due to the nonlinear operation of inverters under partial loading. Overall, the system maintains voltage stability and grid compliance under different irradiance levels, with acceptable THD levels, validating its reliability for varying solar input conditions.

## CONCLUSION

The simulation and performance analysis of a 2 kW, single-phase grid-connected PV system using a T-type multilevel inverter demonstrated effective operation under varying irradiance levels. The implemented MPPT techniques, particularly the fuzzy logic controller, showed superior response time and tracking accuracy compared to traditional methods like P&O and Incremental Conductance. The system maintained stable DC-link voltage and output voltage across all irradiance conditions, while the inverter generated clean multilevel output with acceptable total harmonic distortion levels. Although both voltage and current THD slightly increased under low irradiance, they remained within permissible limits. Overall, the proposed T-MLI-based PV system with advanced MPPT control offers improved efficiency, faster dynamic response, and better power quality, making it a promising solution for residential and small commercial grid-connected solar applications.

## REFERENCES

- [1] Esram, T., & Chapman, P. L. (2007). Comparison of photovoltaic array maximum power point tracking techniques. *IEEE Transactions on Energy Conversion*, 22(2), 439–449.
- [2] Veerachary, M., Senjyu, T., & Uezato, K. (2003). Neural-network-based maximum-power-point tracking of coupled-inductor interleaved-boost-converter-supplied PV system using fuzzy controller. *IEEE Transactions on Industrial Electronics*, 50(4), 749–758.
- [3] Carr, A. J., & Balda, J. C. (2003). A review of current ripple in power converters for battery storage systems. *IEEE Transactions on Industry Applications*, 39(5), 1347–1354.
- [4] Khoucha, F., Lagoun, M. S., Marouani, K., Benbouzid, M. E. H., & Zerguerras, A. (2010). Hybrid cascaded H-bridge multilevel inverter for grid-connected photovoltaic system. *Energy Conversion and Management*, 52(4), 3045–3056.
- [5] Calais, M., Agelidis, V. G., & Borle, L. J. (2001). Multilevel converters for single-phase grid connected photovoltaic systems—An overview. *Solar Energy*, 66(5), 325–335.
- [6] A. Amir, A. Amir, J. Selvaraj, and N. A. Rahim, “Grid-connected photovoltaic system employing a single-phase T-type cascaded H-bridge inverter,” *Sol. Energy*, vol. 199, pp. 645–656, Feb.2020.

- [7] H. P. Vemuganti, R. S. K. Reddy, and A. Deshmukh, "Simulink implementation of Nine-level Cascaded T-type RSC-MLI for 3P3W DSTACOM application," IOP Conf. Ser. Mater. Sci. Eng., vol. 981, no. 4, 2020.
- [8] A. Bughneda, M. Salem, A. Richelli, D. Ishak, and S. Alatai, "Review of multilevel inverters for PV energy system applications," Energies, vol. 14, no. 6, pp. 1–23, 2021.
- [9] L. Hassaine, E. Olias, J. Quintero, and M. Haddadi, "Digital power factor control and reactive power regulation for grid-connected photovoltaic inverter," Renew. Energy, vol. 34, no. 1, pp. 315–321, 2009.
- [10] S. Paghdar, U. Sipai, K. Ambasana, and P. J. Chauhan, "Active and reactive power control of grid connected distributed generation system," Proc. 2017 2nd IEEE Int. Conf. Electr. Comput. Commun. Technol. ICECCT 2017, April, 2017.
- [11] V. K. Sood and H. Abdelgawad, Power converter solutions and controls for green energy. Elsevier Inc., 2019.
- [12] L. Hassaine and M. R. Bengourina, "Control technique for single phase inverter photovoltaic system connected to the grid PV Inverter," Energy Reports, vol. 6, pp. 200–208, Feb. 2020.
- [13] M. Parvez, M. F. M. Elias, N. A. Rahim, and N. Osman, "Current control techniques for three-phase grid interconnection of renewable power generation systems: A review," Sol. Energy, vol. 135, pp. 29–42, Oct. 2016.
- [14] A. Sinha, K. Chandra Jana, and M. Kumar Das, "An inclusive review on different multi-level inverter topologies, their modulation and control strategies for a grid connected photo-voltaic system," Sol. Energy, vol. 170, pp. 633–657, June 2018.
- [15] M. Ciobotaru, R. Teodorescu, and F. Blaabjerg, "Control of single-stage single-phase PV inverter," EPE J. (European Power Electron. Drives Journal), vol. 16, no. 3, pp. 20–26, 2006.
- [16] L. Hassaine and M. R. Bengourina, "Design and digital implementation of power control strategy for grid connected photovoltaic inverter," Int. J. Power Electron. Drive Syst., vol. 10, no. 3, p. 1564, 2019.
- [17] M. Mosa, H. Abu-Rub, M. E. Ahmed, A. Kouzou, and J. Rodríguez, "Control of single-phase grid connected multilevel inverter using model predictive control," Int. Conf. Power Eng. Energy Electr. Drives, pp. 624–628, July 2013.
- [18] C. Boonmee and Y. Kumsuwan, "Control of single-phase cascaded H-bridge multilevel inverter with modified MPPT for grid-connected photovoltaic systems," IECON Proc. (Industrial Electron. Conf.), pp. 566–571, 2013.
- [19] M. BarghiLatran and A. Teke, "Investigation of multilevel multifunctional grid connected inverter topologies and control strategies used in photovoltaic systems," Renew. Sustain. Energy Rev., vol. 42, pp. 361–376, 2015.
- [20] J. Jana, H. Saha, and K. Das Bhattacharya, "A review of inverter topologies for single-phase grid-connected photovoltaic systems," Renew. Sustain. Energy Rev., vol. 72, pp. 1256–1270, Apr. 2017.
- [21] H. Liu, "Control Design of a Single-Phase DC / AC Inverter for PV Applications," pp. 1–5, 2016.
- [22] S. Ray, N. Gupta, and R. A. Gupta, "Active and reactive power management of photovoltaic fed CHB inverter based active filter with improved control under normal/distorted supply," Proc. 2017 12th IEEE Conf. Ind. Electron. Appl. ICIEA 2017, pp. 572–577, Feb 2018.